ISSN: 2319-8753

International Journal of Innovative Research in Science, Engineering and Technology

(An ISO 3297: 2007 Certified Organization)

Vol. 3, Issue 2, February 2014

Study of Concrete under the Action of Hydraulic fracturing in Ⅰ - Ⅱ mixed mode fracture criterion

Mustapha Abdulhadi[1], Sadi Ibrahim Haruna[2] Samir Bashir[3],

Civil Engineering & Architecture College, Liaoning University of Technology, Jinzhou 121001, China [1]

Department of Civil Engineering, Atlim University, Ankara, Turkey [2]

Department of Civil Engineering, Near East University, Nicosia, Cypru [3]

Abstract: This paper simulates the concrete under the action of hydraulic fracturing in Ⅰ-Ⅱ mixed mode fracture. Double-K fracture criterion results in two different loading modes, that is, crack initiation and instability. According to Prefabricated crack and width of the specimen, experimental study of hydraulic fracturing, and the two different loading modes fracture of the specimen were fitted by making the angle formed by the four batches of 24 specimens to be 0°, 30°, 45° and 60° respectively. Axial tensile specimens is applied using hydraulic pressure loading, the crack tip paste the half-bridge strain gages and mounted clip-on extensometer for measurement of crack initiation, extension length and crack opening displacement, the specimen on the two side of water pressure sensor for measuring the extension of the fracture pressure. The total fracture toughness is calculated using overlay method from double-K fracture parameters that is water pressure and axial loads. Study found that, Ⅰ-Ⅱ mixed mode fracture study used two different loading modes component, that is type Ⅰ and Ⅱ fracture component. Under the same angle, $\frac{K_I^{ini}}{K_I^{ini}}$ and $\frac{K_I^{un}}{K_I^{un}}$ are basically the same, and all specimens with prefabricated crack, the crack width decreases with an increase in angle.

Keywords: Include at least 4 keywords or phrases

I. INTRODUCTION

Hydraulic fracturing from the oil and gas industry, with over half a century of development, has been in a wide range of applications such as geotechnical engineering, hydraulic structures etc. Research on hydraulic fracturing is of great important not only for the production and living, but also in possible accident prediction and prevention.

Foreign scholars have done a few relevant studies. Bthuwiler and Saouma [1-2] studied the role of hydraulic fracturing under the pressure in the expansion cracks in the distribution of different sizes in different pressure expansion cracks under pressure distribution; Saouma V [3-5] and others studied the experimental research on the concrete mechanism of hydraulic fracturing, they used the concrete wedge splitting specimens, three different specimens were graded, pilot testing of hydraulic fracturing pressure of the water within the fractures distribution

ISSN: 2319-8753

International Journal of Innovative Research in Science, Engineering and Technology

(An ISO 3297: 2007 Certified Organization)

Vol. 3, Issue 2, February 2014

compared with the numerical simulation; Ito T and Hayashi K [6] carried out rock tri-axial tests on the hydraulic fracturing, which has been in the process of expansion cracks pore water pressure and the crack tip of the three-way relationship between stresses . As hydraulic fracturing research continues to develop, research by china scholars in this area is gradually increasing. Yang You Kui[7] and so on studied a constant flow of water in case the pressure distribution within the fractures were studied, water pressure calculation formula was obtained; Qin Fei, etc. [8] used the finite element method to simulate the crack under the pressure of the water as well as the expansion of the water pressure measurements; Li QingBin and Lin Gao, etc. [9] using special solution boundary element method crack water pressure triangular distribution gravity dam crack stress intensity factor; Zeng KaiHua [10] application of numerical simulation method validation considering the expressions of the principal stress fracturing pressure, hydraulic fracturing verified the destruction of progressive fracturing mechanism; in recent years, Jia Jinsheng, etc. [11] on the assumption that, crack water pressure is uniformly distributed, using the finite element method studies on the ultra-high water pressure crack propagation gravity effects; Wang JianMin, Xu ShiLang [12-14] using wedge-type compact tension specimens in the form of a hydraulic fracture test of concrete under study, using the double K fracture model of its unstable fracture toughness, toughness and cohesive crack initiation toughness, fracture toughness from its measured and calculated values were compared.

II. EXPERIMENTAL METHADOLOGY

This paper focuses on the study of Ⅰ-Ⅱ mixed mode fracture, according to the pre-slit width of the specimen, two kinds of fracture forms were simulated by making the angle formed by four batches of 24 specimens to be 0 °, 30 °, 45 ° and 60 ° respectively, as shown in Fig. 1-4, and the dimension as shown in Table 1. The experiment was carried out using ordinary disposable C30 concrete, and the ratio of cement, sand, gravel and water were 1: 1.32: 3.06: 0.5 respectively. Huludao Bohai Cement Co., Ltd. used the PSA32.5 of slag cement, coarse aggregate which maximum particle size does not exceed 25mm of gravel, fine aggregate particle less than 5mm of natural medium sand and water.

TABLE 1

PARAMETERS OF THE SPECIMEN

Length L（mm）	**Width W（mm）**	**High H（mm）**	**Crack length a（mm）**	**Crack depth h（mm）**
900	600	450	130	350

The active forces of the test include axial force and water pressure. Axial force applied by hydraulic jack; water pressure provided by an electric hydraulic pump as shown in Figure 5. In order to achieve the pressure applied and sealed state, the screw and the cover of the extrusion pressure were embedded around the crack 8 screw, to achieve a sealed, water and exhaust ports were at the top of the cover. Test crack tip by attaching the half-bridge strain gauge as shown in Fig. 6, the tip of the strain measured changes in joints. In order to cover the multilayer mat rubber gasket,

ISSN: 2319-8753

International Journal of Innovative Research in Science, Engineering and Technology

(An ISO 3297: 2007 Certified Organization)

Vol. 3, Issue 2, February 2014

gaskets butter plus a painted cement mixture were used. Trials were in the pre-sewn seam at the tip and clip-on extensometer was used to measure the crack tip opening displacement and transforms the situation. Both ends of the specimen through the water pressure sensor measured water pressure and crack propagation. A pressure sensor shown in Fig. 7 and a hydraulic jack are used to connect the specimen and measure the axial load values.

Loading test was in two ways:

(1) Water pressure was applied to the case at a constant axial force;

(2) A constant axial force was applied under pressure.

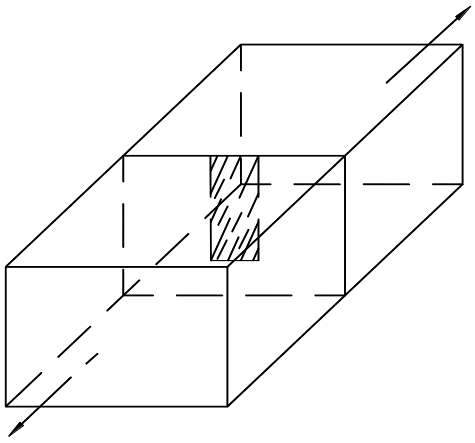

Fig.1 The schematic diagram of the axial tension specimen with 0°degree

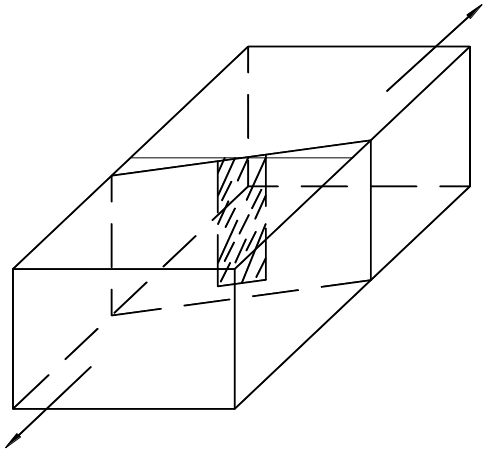

Fig. 2 The schematic diagram of the axial tension specimen with 30°degree

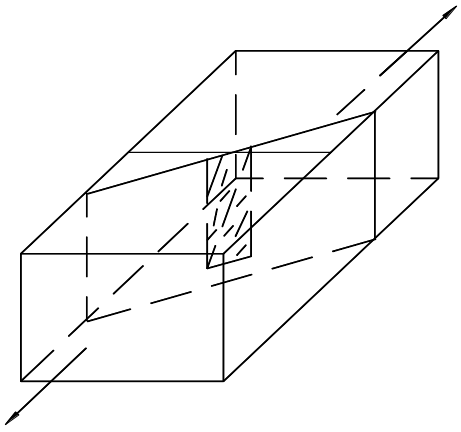

Fig. 3 The schematic diagram of the axial tension specimen with 45°degree

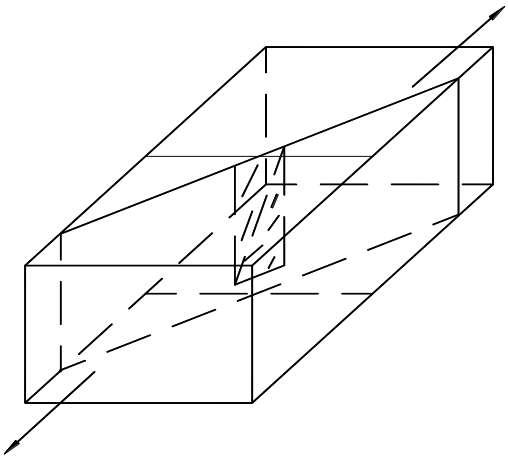

Fig. 4 The schematic diagram of the axial tension specimen with 60°degree

ISSN: 2319-8753

International Journal of Innovative Research in Science, Engineering and Technology

(An ISO 3297: 2007 Certified Organization)

Vol. 3, Issue 2, February 2014

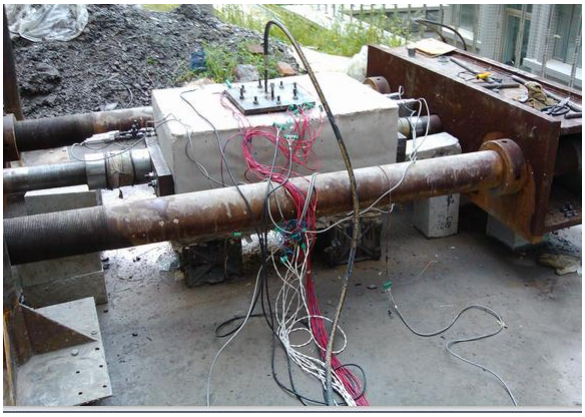

Fig.5 Test loading device

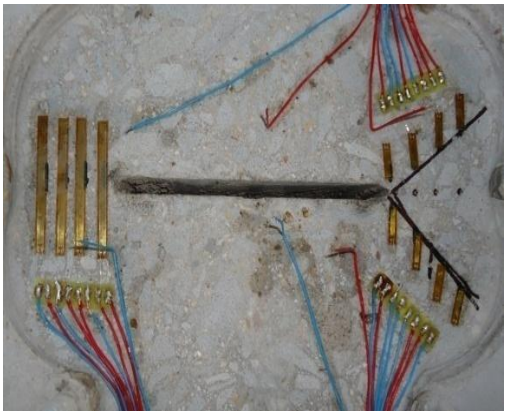

Fig.6The Strain gauges' arrangement

Fig. 7 axial force sensor

Double-K fracture theory as the whole process can be divided into crack initiation, crack propagation and crack instability. Application of the theory of double-K fracture is the key to the whole process of fracture to determine the crack point and instability point. A lot of trials found that the fracture process of crack initiation point is the P-CMOD curve rises linear to nonlinear phase transition point; instability point is the point of peak load in the curve.

A. Experimental determination of crack initiation toughness

Determining the fracture toughness of the crack initiation is the key to determine the load from the main methods for crack test, that is, curve inflection point method, half-bridge and full-bridge assay method. Many experimental studies have shown that, in determining the crack initiation point, it is often not easy to determine linear and nonlinear turning point, the choice is often caused by a large human error, so this test was used to determine the half-bridge assay, initiation point through the crack tip strain gauges. From the beginning, precast concrete crack tip began to gathered energy, so the test load-strain curve had increased to extremes upward trend and started retraction, which resulted in the appearance of cracks, the aggregation energy began to be released, measuring point was unloaded, the strain began to restored the previous value of the load when the load was at the point of the crack initiation, so in this case the crack tip

ISSN: 2319-8753

International Journal of Innovative Research in Science, Engineering and Technology

(An ISO 3297: 2007 Certified Organization)

Vol. 3, Issue 2, February 2014

strain gauge full bridge of the crack fracture load is the whole process of load initiation [15] - [16]. Crack load from the load based on cutting-edge signifies that - a strain curve is determined, Fig. 4.

（1） fracture specimens：

$$K_I^{ini} = P_{ini}\sqrt{\pi a}\cdot F_I(\alpha,\beta) \qquad K_{II}^{ini} = 0 \quad \text{……..} \quad (1)$$

（2） I-II mixed mode fractures specimens：

$$K_I^{ini} = F_I \cdot P_{ini}\sqrt{\pi a}$$

…… …… (2)

$$K_{II}^{ini} = F_{II} \cdot P_{ini}\sqrt{\pi a}$$

As the pilot is in pressure, an external loads carried out under the joint action of the initial fracture toughness from the outside loads initiation fracture toughness and the crack under pressure superposition of fracture toughness.

$$K_I^{ini} = K_{I\,ini}^{L} + K_{I\,ini}^{W} \quad \text{……} \quad (3)$$

$$K_{II}^{ini} = K_{II ini}^{L} + K_{II ini}^{W} \quad \text{……} \quad (4)$$

Where,

K_I^{ini} Represents initiation fracture toughness type Ⅰ;

K_I^{ini} Represents initiation fracture toughness type Ⅱ;

$K_{I\,ini}^{L}$ Represents initiation fracture toughness for the axial force type Ⅰ;

$K_{I\,ini}^{W}$ Represents initiation fracture toughness for the water under pressure type Ⅰ;

$K_{II\,ini}^{L}$ Represents the fracture toughness for the axial force from the crack under the type Ⅱ;

$K_{II\,ini}^{W}$ Represents the fracture toughness for the water under pressure type Ⅱ;

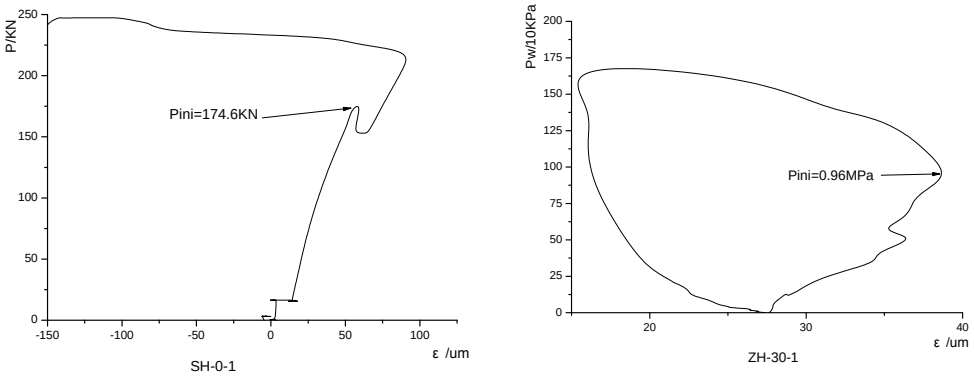

Fig.8 load (at the crack) – strain relationship

ISSN: 2319-8753

International Journal of Innovative Research in Science, Engineering and Technology

(An ISO 3297: 2007 Certified Organization)

Vol. 3, Issue 2, February 2014

B. Experimental determination of unstable fracture toughness

Fracture toughness is composed of two parts: the axial loads and loads of water instability under pressure, which is calculated from the total superimposed unstable fracture toughness and it is determined based on P-CMOD curve rising section, Fig. 4.

Because crack instability has been completed in the expansion phase, the crack length becomes the initial crack length and the length of the crack propagation. Measurement of the extended length of the test method was as follows: initially, the strain continued to accumulate as the load increased linearly with increasing energy, after reaching the maximum strain, the strain began to retracted, the energy is released, which showed that, strain gage crack had been extended to the maximum strain value corresponding to the load, that is, the crack extension load value, for which we can monitor each of the strain gauge crack extension process until the fracture specimen is unstable.

（1）fracture specimens：

$$K_{I}^{\mathrm{un}} = \mathrm{P}_{\mathrm{un}}\sqrt{\pi(a+\Delta a)}\cdot F_{I}(\alpha,\beta) \qquad K_{II}^{\mathrm{un}} = 0 \quad \text{……（5）}$$

（2）I-II mixed mode fractures specimens：

$$K_{I}^{\mathrm{un}} = F_{I}\cdot \mathrm{P}_{\mathrm{un}}\sqrt{\pi(a+\Delta a)}$$

$$K_{II}^{\mathrm{un}} = F_{II}\cdot \mathrm{P}_{\mathrm{un}}\sqrt{\pi(a+\Delta a)} \quad \text{……（6）}$$

Where,

$F_{I}(\alpha,\beta)$， F_{I}， F_{II} are "stress intensity factors" corresponding value found in Handbook

$(a+\Delta a)$ The total length of crack extension after crack

Similarly, the fracture toughness was considered unstable fracture total axial force and the combined effect of water pressure for the superposition of unstable fracture toughness were obtained:

$$K_{I}^{\mathrm{un}} = K_{I\,\mathrm{un}}^{\mathrm{L}} + K_{I\,\mathrm{un}}^{\mathrm{W}} \quad \text{……（7）}$$

$$K_{II}^{\mathrm{un}} = K_{II\mathrm{un}}^{\mathrm{L}} + K_{II\mathrm{un}}^{\mathrm{W}} \quad \text{……（8）}$$

Where,

K_{I}^{un} Represent unstable fracture toughness type I;

K_{II}^{un} Represents unstable fracture toughness type II;

$K_{I\,un}^{L}$ Represents unstable fracture toughness for the axial force of type I;

$K_{I\,un}^{w}$ Represents unstable fracture toughness for the water under pressure type I;

$K_{II\,un}^{L}$ Represents unstable fracture toughness for the axial force of type II;

$K_{II\,un}^{w}$ Represents unstable fracture toughness for the water under pressure type II;

ISSN: 2319-8753

International Journal of Innovative Research in Science, Engineering and Technology

(An ISO 3297: 2007 Certified Organization)

Vol. 3, Issue 2, February 2014

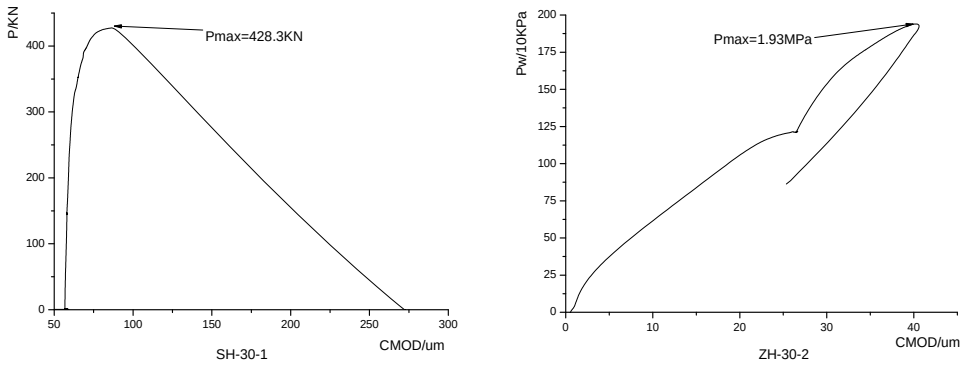

Fig.9 Curves of load-crack mouth opening distance

III. TEST RESULTS

Test results are shown in Table 2.

TABLE 2

RESULTS OF FRACTURE PARAMETERS

No.	(MPa $m^{\frac{1}{2}}$)		(MPa $m^{\frac{1}{2}}$)		(MPa $m^{\frac{1}{2}}$)		(MPa $m^{\frac{1}{2}}$)		K_I^{ini} (MPa $m^{\frac{1}{2}}$)	K_I^{ini} (MPa $m^{\frac{1}{2}}$)	K_I^{un} (MPa $m^{\frac{1}{2}}$)	K_I^{un} (MPa $m^{\frac{1}{2}}$)
SH-0-1	0.605	Pure	0.842	Pure	0.853	Pure	0.674	Pure	1.447	Pure	1.527	Pure
SH-0-2	0.770	type	0.739	type	0.849	type	0.487	type	1.509	type	1.336	type
SH-0-3	0.558	I	0.370	I	1.019	I	0.314	I	0.928	I	1.333	I
Aver	0.644		0.650		0.907		0.483		1.295		1.399	
ZH-0-1	0.825	Pure	0.496	Pure	0.825	Pure	0.941	Pure	1.321	Pure	1.739	Pure
ZH-0-2	0.867	type	0.197	type	0.887	type	0.866	type	1.064	type	1.753	type
Zh-0-3	0.701	I	0.505	I	0.701	I	0.646	I	1.206	I	1.347	I
Aver	0.798		0.399		0.804		0.818		1.197		1.613	
SH-301	0.381	0.214	0.514	0.289	1.167	0.628	0.489	0.275	0.895	0.503	1.656	0.903
SH-302	0.372	0.209	0.669	0.376	1.181	0.665	0.352	0.198	1.041	0.585	1.533	0.863
SH-303	0.370	0.208	—	—	1.254	0.705	—	—	—	—	—	—
Aver	0.374	0.210	0.592	0.333	1.201	0.666	0.421	0.237	0.968	0.544	1.595	0.883
ZH-301	0.641	0.360	0.345	0.194	0.647	0.364	0.591	0.333	0.986	0.554	1.238	0.697
ZH-302	0.561	0.315	0.429	0.242	0.561	0.315	0.679	0.382	0.99	0.557	1.240	0.697
ZH-303	0.970	0.546	0.092	0.052	0.873	0.491	0.528	0.297	1.062	0.598	1.401	0.788
Aver	0.724	0.407	0.289	0.163	0.694	0.400	0.599	0.337	1.013	0.570	1.293	0.727
SH-451	0.394	0.384	0.378	0.368	—	—	—	—	0.772	0.752	—	—
SH-452	0.446	0.435	0.359	0.350	0.624	0.608	0.354	0.345	0.805	0.785	0.978	0.953
SH-453	0.402	0.392	0.378	0.368	0.411	0.400	0.378	0.368	0.780	0.760	0.789	0768
Aver	0.414	0.404	0.372	0.362	0.518	0.504	0.366	0.357	0.786	0.766	0.908	0.861
ZH-451	0.390	0.380	0.132	0.129	0.390	0.380	0.321	0.313	0.522	0.509	0.711	0.693

ISSN: 2319-8753

International Journal of Innovative Research in Science, Engineering and Technology

(An ISO 3297: 2007 Certified Organization)

Vol. 3, Issue 2, February 2014

ZH-452	0.306	0.298	0.260	0.253	0.306	0.298	0.531	0.518	0.566	0.551	0.837	0.816
ZH-453	—	—	—	—	—	—	—	—	—	—	—	—
Aver	0.348	0.339	0.196	0.191	0.348	0.339	0.426	0.416	0.544	0.530	0.774	0.755
SH-601	0.101	0.170	0.238	0.402	0.172	0.291	0.230	0.388	0.339	0.572	0.402	0.679
SH-602	0.175	0.296	0.164	0.277	0.356	0.601	0.113	0.191	0.349	0.573	0.469	0.792
SH-603	0.201	0.339	0.131	0.221	0.220	0.372	0.131	0.221	0.332	0.560	0.351	0.593
Aver	0.159	0.268	0.178	0.300	0.249	0.421	0.158	0.267	0.340	0.568	0.407	0.688
ZH-601	0.196	0.331	0.292	0.492	0.196	0.331	0.321	0.543	0.488	0.823	0.517	0.874
ZH-602	0.176	0.298	0.203	0.344	0.176	0.298	0.309	0.523	0.379	0.642	0.485	0.821
ZH-603	—	—	—	—	—	—	—	—	—	—	—	—
Aver	0.186	0.315	0.248	0.418	0.186	0.315	0.315	0.533	0.434	0.733	0.501	0.848

SH represents the case of a constant pressure; ZH represents added axial force under constant pressure; 60, 45, 30, 0 are the angle between the specimen width and the preformed slit; 1, 2, and 3 represents the specimen number.

The results showed that, under the same angle, $\frac{K_I^{ini}}{K_I^{ini}}$ and $\frac{K_I^{un}}{K_I^{un}}$ are basically the same, and are sewn with the preformed angle of the test. The results are fitted to the curve shown in Fig.10;

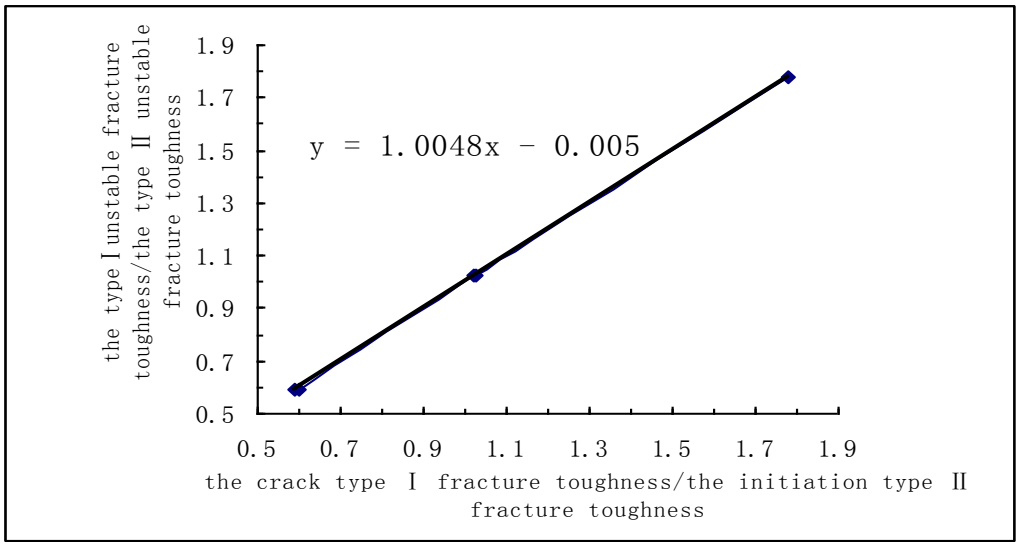

Fig 10 Fitting Curve of $\frac{K_I^{ini}}{K_I^{ini}}$ and $\frac{K_I^{un}}{K_I^{un}}$

The mathematical expression for the result in table 2 is summarize in table 3 and the fitting curve of I-II mixed mode fracture is plotted, as in fig. 11-12.

ISSN: 2319-8753

International Journal of Innovative Research in Science, Engineering and Technology

(An ISO 3297: 2007 Certified Organization)

Vol. 3, Issue 2, February 2014

TABLE 3

MATHEMATICAL EXPRESSIONS OF I-II MIXED MODE CRITERION

Test load type		Fitting equation
Constant water pressure add axial force	Initiation toughness curve fitting	K_{II}^{ini}=-0.5544$\left(K_I^{ini}\right)^2$+0.4249K_I^{ini}+0.5315
	Unstable fracture toughness curve fitting	K_{II}^{un}=-0.1203$\left(K_I^{un}\right)^2$−0.111K_I^{un}+0.8716
Constant axial force add water pressure	Initiation toughness curve fitting	K_{II}^{ini}=-0.3675$\left(K_I^{ini}\right)^2$−0.1245K_I^{ini}+0.8851
	Unstable fracture toughness curve fitting	K_{II}^{un}=-0.4056$\left(K_I^{un}\right)^2$+0.1565K_I^{un}+0.9941

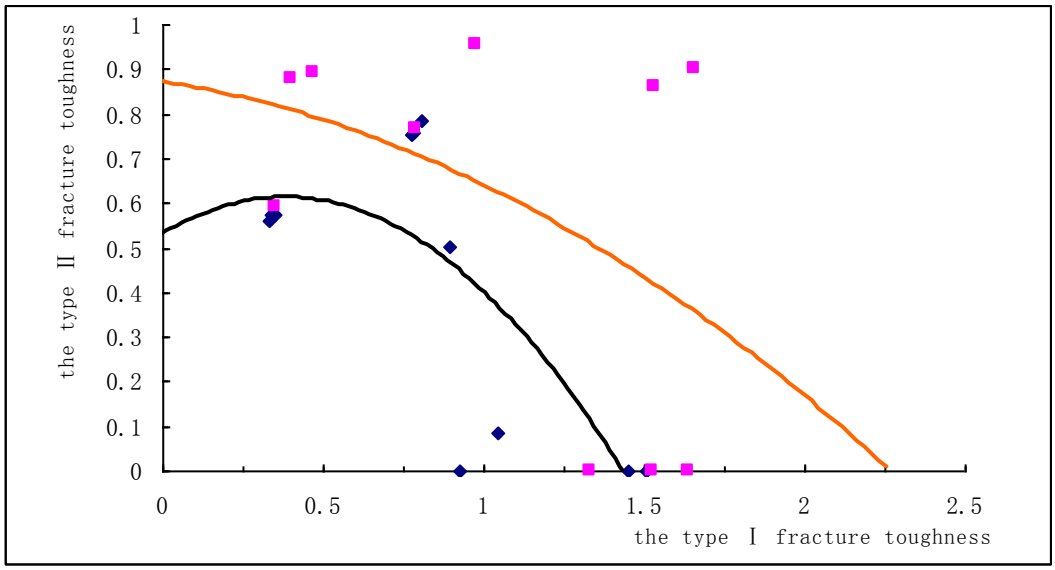

Fig.11 The fitting curves of I-II mixed mode fracture to maintain water pressure

ISSN: 2319-8753

International Journal of Innovative Research in Science, Engineering and Technology

(An ISO 3297: 2007 Certified Organization)

Vol. 3, Issue 2, February 2014

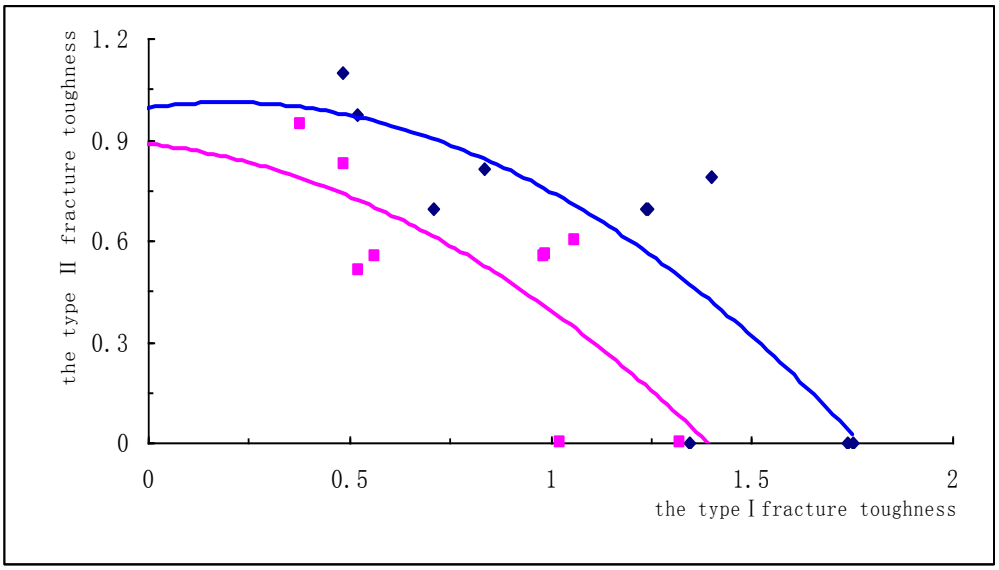

Fig.12 the fitting curves of I-II mixed mode fracture to maintain the mechanical load

IV. CONCLUSION

The following conclusions could be drawn from the present investigation-

(1) It is observed that, the fracture toughness is calculated from the total demand superimposed fracture toughness by taking into account the axial load and water pressure.

(2) Double-K fracture criterion was applied in the calculation of crack initiation and unstable fracture toughness. Two different loading modes, that is, initiation and unstable fracture toughness are compared in both loading and stability lost of the fracture criterion.

(3) I-II mixed mode fracture study used two loading modes type; I fracture components (initiation fracture toughness type I and unstable fracture toughness type I) are sewn with the prefabricated specimen with the width decreases with an increase in angle, II fracture components (initiation fracture toughness type II and unstable fracture toughness type II) are sewn with the prefabricated specimen, with the width increases. Under the same angle $\frac{K_I^{ini}}{K_I^{ini}}$ and $\frac{K_I^{un}}{K_I^{un}}$ are basically the same, and in both cases, width decreases with an increase of angle.

REFERENCES

[1] Bruhwiler E,Saouma V.Water fracture interaction in concrete, Part II:hydrostatic pressure cracks[J].ACI Materials Journal,1995,92(4):383-390.

[2] Volker V, Saouma V. Water pressure in propagating concrete cracks[J].Journal of Structure Engineering,2000,126(2):235-242.

[3] Bruhwiler E ,Saouma V.Water fracture interaction in concrete ,Part I :fracture properties [J].ACI Materials Journal,1995,92(3):296-303.

[4] Bruhwiler E,Saouma V.Water fracture interaction in concrete, Part II:hydrostatic pressure cracks[J].ACI Materials Journal,1995,92(4):383-390.

[5] Volker V, Saouma V. Water pressure in propagating concrete cracks[J].Journal of Structure Engineering,2000,126(2):235-242.

ISSN: 2319-8753

International Journal of Innovative Research in Science, Engineering and Technology

(An ISO 3297: 2007 Certified Organization)

Vol. 3, Issue 2, February 2014

[6] Ito T,Hayashi K.Analysis of crack reopening behavior for hydrofrac stress measurement[A]. Haimson B. Rockmechanics in 1990s:Pre2p rant proceedings of the 34 the U.S. Symposium on Rock Mechanics[C].Madison: University of Wisconsin2 Madison,1993.335-338.

[7] Yang Youkui, Xiao Changfu, Qiuxian De, Wu Gang. hydraulic fracture morphology and seam pressure distribution. Journal of Chongqing University (Natural Science Edition), 1995,18 (3) :20-26.

[8]Qin Fei, Li Ying. Crack under the water pressure boundary element analysis. Engineering Mechanics, 2003 Suppl :304-307.

[9] Li Qingbin, Lin Gao, Zhou Hongjun. Different elastic modulus Boundary Element Analysis of Interfacial Crack in its application. Dalian University of Technology, 1991, (02) :199-204.

[10] Zeng Kaihua, Yin Zongze. Earth core dams hydraulic fracturing influencing factors [J]. Hehai University, Vo1, No.3, 2000, 28PP.1-6.

[11] Jia Jinsheng, Li Xinyu, Zheng Cuiying. Especially considering the high pressure water splitting effect gravity preliminary study. Journal of Hydraulic Engineering, 2006 (12) :1509-1515.

[12] Xu ShiLang, Wang Jianmin. Concrete dam cracks under water pressure expansion and double-K fracture parameters [J]. Civil Engineering Journal, 2009,42 (2) :119-125.

[13] Wang Jianmin, Xu ShiLang. Experimental study on fracture of concrete under water pressure [J]. Construction Technology, 2011,40 (342) :43-47.

[14] Xu ShiLang, Wang Jianmin. Concrete under hydrostatic pressure test measures the double K fracture parameters [J]. Hydraulic Engineering, 2007,38 (7) :23-32.

[15] Zheng Shuang. Many cracks in concrete specimen geometry of static stress intensity factor: (Master Thesis). Liaoning: Dalian University of Technology, 2005.

[16] Karihaloo, B.L. and Nallathambi, P.. Effective Crack Model for the Determination of Fracture Toughness KIcs of Concrete. Engineering Fracture Mechanics,1990, 35(4/5):637-645.